



TURBO-MACHINERY DESIGN BASED ON MULTI-PHYSICS FLUID-STRUCTURE OPTIMIZATION

Kossivi GOKPI¹, Jacques MARCHESINI¹
Bruno DEMORY², Manuel HENNER²

¹ *INTES FRANCE, 40, Rue Sardi Carnot. 78120 Rambouillet, France*

² *VALEO, Thermal Systems, 8 Rue Louis Lormand, CS 80517, La Verrière.
78322 Le Mesnil Saint-Denis, France*

SUMMARY

This paper aims to show the geometric parameterization of a fan and the mesh morphing capability used during a numerical DoE (Design of Experiment). Static deformations under centrifugal effect, eigenmodes and their resulting displacements are predicted for 900 combinations of the 12 geometrical parameters. Investigations have shown that the aerodynamic steady loading can strongly modify the blade deflection whereas the flow unsteadiness is barely affecting the modes. Results are used to evaluate the set of parameters that influence the structural deformation of the blades and which are relevant for a multi-physic optimization process.

INTRODUCTION

Significant research efforts are being undertaken by OEM (Original Equipment Makers) and their suppliers to improve the energy performance of our cars. In the thermal domain, one intend of engineers is to provide more efficient cooling modules, which can save energy thanks to a low impact on the vehicle drag and with a reduced electrical consumption for fan systems. These energy saving prospects lead to increased research and development efforts in the field of ventilation. Numerical means are widely used for the optimization of fans according to the best compromise between efficiency, acoustics, mechanical robustness and packaging. CFD and FEA are therefore widely used, and methodologies are set up to accelerate the simulation turn-over during Design of Experiment (DoE) or iterative optimization loops.

In order to explore these methodologies, several academic and industrial partners have joined forces as part of a research consortium supported by the French National Research Agency (ANR). Purpose of this project is to experiment large-scale experimental design techniques (up to

60 parameters) and its implementation with intensive and multi-physics simulations. This project, whose acronym is PEPITO (in French “Plan d’Expérience pour l’Industrie du Transport et l’Optimisation”, i.e. Design of Experiment for the Transport Industry and Optimization) includes tasks related to the development of computational processes that can be used while performing DoE [1]. Therefore numerous simulations have to be launched and a full automation from the initial set-up until the post-processing is required. The parameterization should allow a wide exploration of the solution domain through geometrical factors that describe the geometry, or physical factors that represent the operating conditions.

Previous works have assessed the quality of the aerodynamic and aeroacoustic predictions that are used in the frame of the PEPITO project. Published results have shown that performances in terms of pressure and torque are correctly evaluated by CFD [2], whereas acoustic predictions are producing approximate values that can be used only in global trends [3]. These methods are based either on analytical models using Amiet’s theory, or on propagation according to the FW&H method of source terms evaluated during an URANS calculation. Other methods based on LES (Large Eddy Simulation) or LBM (Lattice Boltzmann Method) are considered so far too expensive in term of CPU usage for the objective of large DoE.

Following these previous studies, the content of this article aims to present the work conducted for parameterization and simulation coupling between CFD and FEA for predictions of structural deformation and modal analysis.

OBJECTIVES

The goal of this work is to experiment a simulation process aimed to fulfill the requirements of intense simulation campaigns during fan development. The techniques used combine the following methods to be tested:

- a geometric parameterization according to turbomachine design rules
- a morphing technique for the FEA mesh, allowing all parameter combinations
- a coupling between CFD and FEA to take into account stationary and unsteady loading
- an automation of simulation runs and post-processing

Several results are related to the checks carried out to assess the quality and relevance of the method. Technical aspects considered are:

- Verification of the mesh quality, as the deformation propagation must not lead to cell crushing or overturning
- Cost estimation of the method which must be compatible with the objective of performing large DoE with many runs
- Post-processing of structural analysis for deformation or eigenmodes, and sensitivity analysis of the parameters for each output
- Comparison of results according to whether the coupling uses the unsteady loading or not

This paper deals with these topics through the various paragraphs that present the parameterization for the fan, the morphing technique, the influence of the aerodynamic loading and initial results with sensitivity analysis. Conclusions and perspectives are then delivered.

FAN PARAMETERISATION

One of the first steps in the project was to define common parameters that could be used for all cases to be simulated whatever the physic, and for the statistical analysis of data, whether for factors or responses. The original DoE plan originally includes 15 factors, one of them being a physical parameter which imposes the operating point (i.e. mass flow rate). Two other factors are related to distance and diameter of the plate located downstream the fan and aimed to represent the engine

blockage in the underhood (figure 1). While these values may be important for aerodynamics, they were initially neglected for structural calculation. Of the remaining 12 parameters, 4 are devoted to the description of 4 chord length at 4 different radii (figure 2), 4 are for stagger angles, 2 for the blade camber and 2 for the blade sweep (figure 3). The rotor is constituted of 7 blades. In this specific case the blade is subdivided into 5 equidistant sections named R1 to R5. R1 is the section connected to the hub and R5 is the section connected to the ring. Table 1 shows the details of the airfoil section where a variable is defined in the design of experiment corresponding to the sections shown in figure 2.

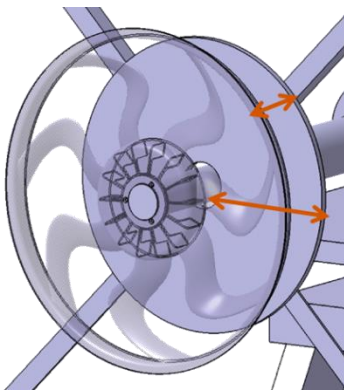


Figure 1: Example of one case showing the fan and its context

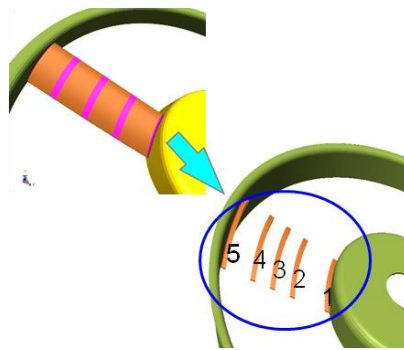


Figure 2: 4 blade spans to describe profile

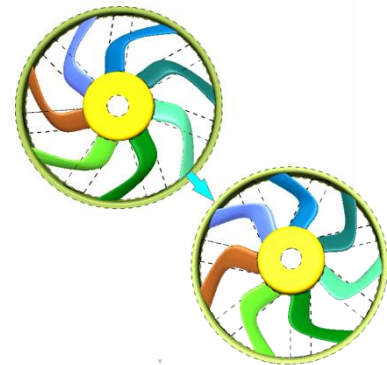


Figure 3: example of stacking variation by morphing

Table 1: geometrical parameters in the design of experiment

Variable Name	Airfoil sections on which the variables is parameterized
Chord	R1, R2, R4, R5
Stagger angle	R1, R2, R4, R5
Camber	R1, R2
Sweep Angle	R3, R5

MESH MORPHING

Mesh morphing methods are widely proposed for their ability to speed-up iterative simulation processes. They have a great interest for fluid-structure interaction as it was shown by Rozenberg & al [4]. As the mesh properties like density or connectivity remains unchanged, previous results can be mapped quite easily and used for simulation restart, which is obviously very important for strong coupling.

The software PERMAS used for these study is going further by using this technique even for large displacement (figure 3). On the base of the parameters described previously, a geometrical deformation is calculated and applied on a set of nodes from the surfaces or the edges. The modeling of the geometric factors for the blade is done in the GUI of VisPER [5] (the visualization tool of the FEA software PERMAS). The five selected profiles are used to guide the geometric

morphing along 17 intermediate sections (figure 4), their displacements being done according to the common parameterization process previously presented.

This deformation is then propagated with PERMAS [5] in the volume according to an algorithm which takes into account distances from moved surfaces. Radial based functions as presented by De Boer & al [6] are often used as they allow smoothing the deformation inside the domain. In addition, some rules must be applied to isolate non deformable shapes (like the hub) and to maintain some geometrical characteristics like a constant radius and a constant axial position for the 5 selected spans. As the software accepts non-conformal meshes without accuracy issue, and since all the geometrical parameters are defined on the blade profiles, both variations of the ring and the hub heights are deduced from the profile dimensions at bottom and top (figure 5).

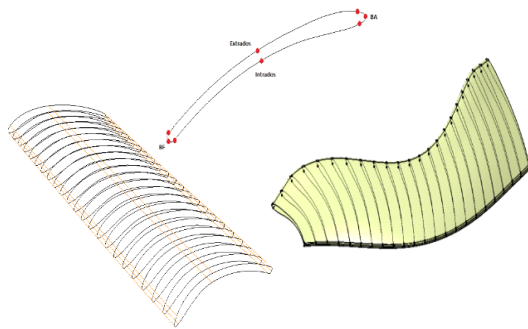


Figure 4: Airfoil sections for parameterization

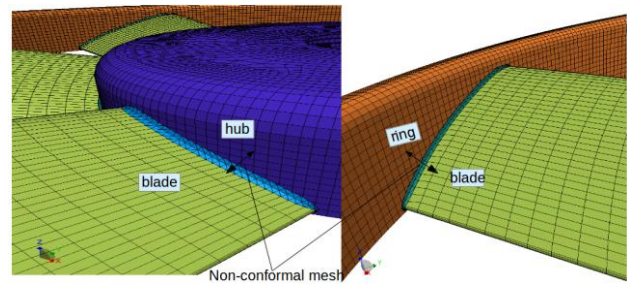


Figure 5: Mesh morphing with the capability of handling non-conformal mesh

FAN DEFORMATION AND MODAL ANALYSIS

It is then possible to establish sets of parameters and to quickly conduct numerous simulations having all the same mesh quality and resolution. In the present study, the total cells number of the finite element model is 87534, whatever the morphed geometry. An example are shown in figure 6 the morphing with maximal sweep at mid span, the resulting static deformation under operation and the pumping mode.

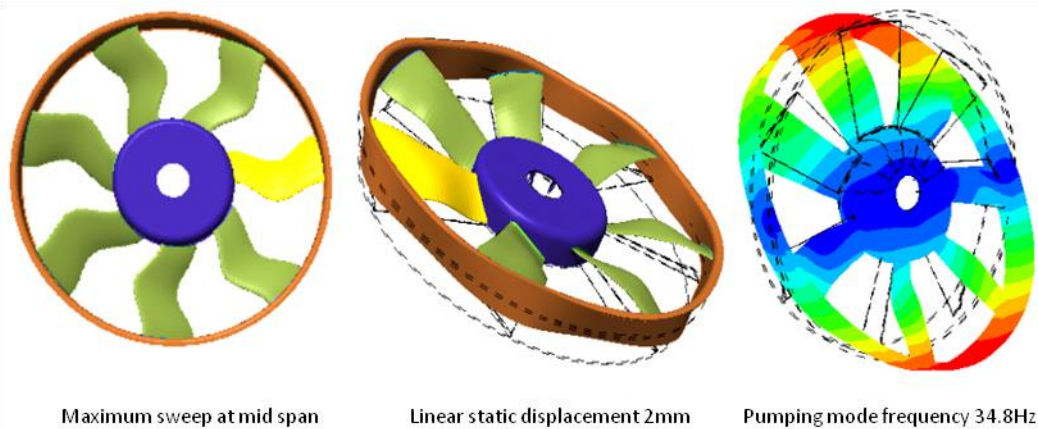


Figure 6: Mesh morphing example for sweep parameter with modal analysis under centrifugal loading, at 2500 rpm

SIMULATION WITH FLUID-STRUCTURE INTERACTION

A first study was conducted to establish the methodology aimed to take into account the fluid structure interaction. It also shows the rotordynamics simulations and capability of the finite elements software PERMAS [7, 8 and 9]. To this end, a first aerodynamic simulation was carried out using the open source code OpenFOAM [10], and the results were used as an input for the effect of air pressure during structural calculations with Permas.

CFD Validation: aerodynamic performances

The fan performances are predicted numerically in a simple configuration of test rig without any obstacle like heat exchanger or stator vanes (see [2]). Rotor diameter is 423 mm, 7 blades are distributed symmetrically around the hub and are attached to their tip by a rotating ring (figure 7). For simulation, rotating speed is set at 2500 rpm and five different flow rates are imposed as inlet boundary condition. (800, 1600, 2800, 4000 and 5200 m³/h).

Steady and unsteady CFD numerical simulations are performed with the open source code OpenFOAM (version 2.31), using tetrahedral cells (about 7 millions) and extruded mesh on walls to provide a Y^+ close to 1. The RANS analysis was performed with second order schemes in space, using a two equations $k-\epsilon$ realizable turbulence model. A MRF (Multi Reference Frame) model is adopted for the steady simulation of the rotor motion, while for the unsteady CFD simulation a dynamic mesh moving model was used with the second order time step solver. Residuals and stabilities of global performances (pressure and torque) are monitored during simulation in order to ensure a good convergence. 13 rotations were needed to reach a good convergence and 6 more rotations have been done for the post-processing of global performances.

Figure 8 presents as example, a post-processing of the velocity magnitude in a plane parallel to the axis of rotation. For this flow rate (i.e. 2800 m³/h) the flow pattern is rather axial and velocities are higher close to blade tip.



Figure 7: Fan in his rotating domain

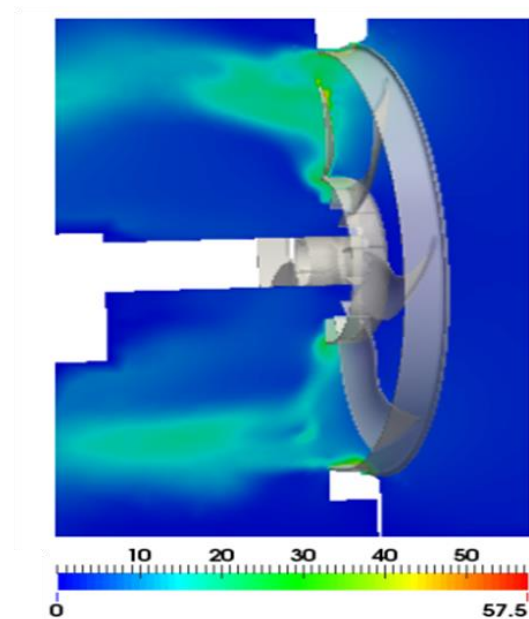


Figure 8: velocity fields at rear the rotor at flow rate of 2800 m³/h

Figure 9 shows the pressure distribution of both side of the fan, i.e. upstream for the suction sides of blades and downstream for the pressure side. The post-processing done for this nominal operating point (i.e. 2800 m³/h) demonstrates the rather good quality of the fan design since the whole blade span is correctly loaded, except close to the hub. This phenomenon is well known for large diameter fan: the low aerodynamic loading results in a low pressure area at blade bottom, whereas flow separation close to trailing edge occurs on upper side at lower radii.

In figure 10 is shown a comparison of global performance (pressure drop and torque) between steady, unsteady simulation and experimental data. One can observe that CFD results match globally well with experiment, and discrepancies are quite limited for the torque prediction at low flow rates with steady simulations. Reasons for these differences have not been investigated in this work, and it will just be noted that the simulation does not correctly predict effects of a high flow incidence on the blade (i.e. when flow rates are low).

These results are, however, satisfactory in the context of the present study, since the main objective is to assess the actual load seen by the blade during operation. Steady or unsteady results for pressure loading can be considered to be both enough close to reality for the fluid structure interaction.

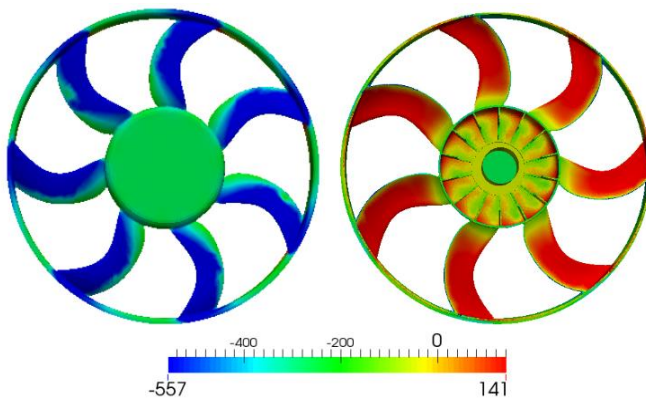


Figure 9: From left to right : Pressure distribution on suction side (left) and pressure side (right) of fan blades

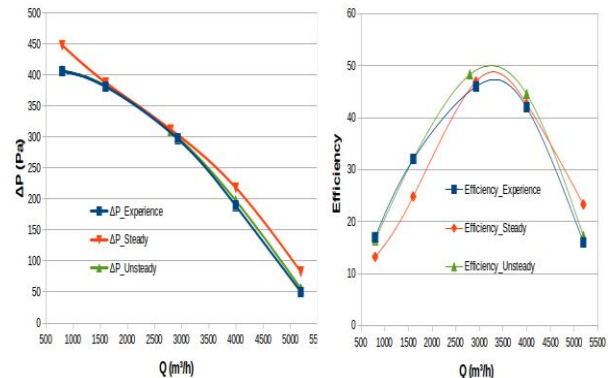


Figure 10: Comparison of CFD and experimental results for pressure drop (total-to-static) and efficiency

Fluid-structure simulation: linear static deformation and modal analysis

The fluid-structure calculation uses the extracted aerodynamic pressure combined with the centrifugal force as a load for structural analysis. This will allow evaluating and comparing the contribution of each load (pressure or centrifugal) in the determination of the linear static deformation. The fluid-structure procedure is also put in place to demonstrate the coupling capability of structure software Permas with the CFD open source software OpenFOAM [11, 12].

Figure 11 shows the displacement field of the static linear deformation of the rotor under centrifugal force, pressure force and their combination. With pressure load only, the maximal axial displacement is +2.17 mm, meaning that the fan is pushed upstream in the axial direction by the pressure. Considering centrifugal force only results in a displacement in the reverse direction by -1.25 mm. The resulting axial displacement is 1.27 mm when combining the loads of pressure and centrifugal force.

It's noticeable that the pressure load has a significant influence on the rotor linear deformation and it's relevant to take it into account when designing the rotor-stator system.

Figure 12 shows the deformation of the first frequency modes with pressure or centrifugal loading, and for their combination. The first row shows the modal frequency analysis without any load. The

second row shows the modal frequency analysis of the rotor constrained with the centrifugal load. The frequencies significantly change and this shows the impact of the centrifugal effect on the rotor. Since the centrifugal force introduces more rigidity in the structure, thus the frequencies of modes increase. While loading the aerodynamic pressure load combined with the centrifugal the frequencies did not change significantly from the centrifugal mode frequencies. Only the pumping mode (first mode) has shifted slightly. This information is showing that for modal analysis in rotor dynamics, the pressure load did not play a significant role on the frequencies of the modes.

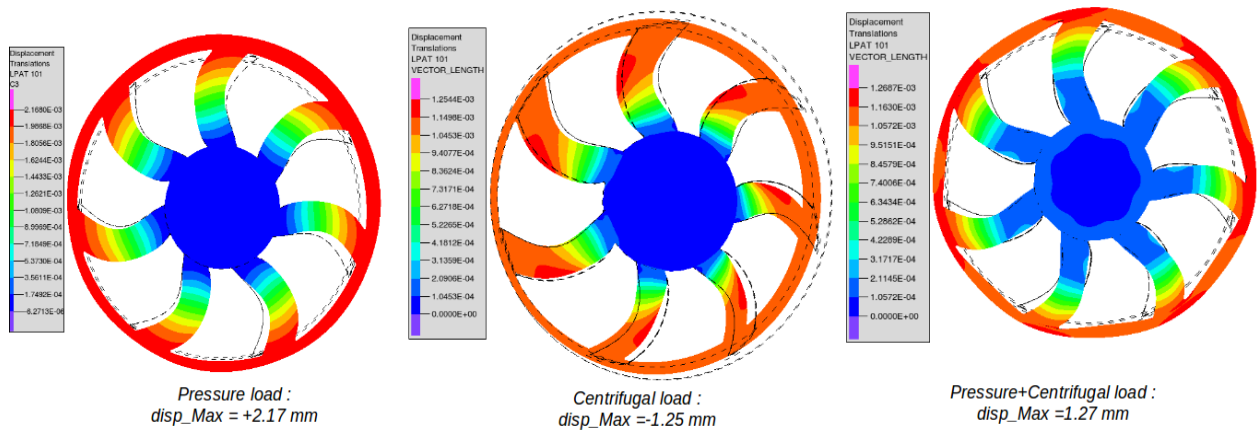


Figure 11: From left to right: Maximal axial linear static deformation with pressure load, rotating load and both

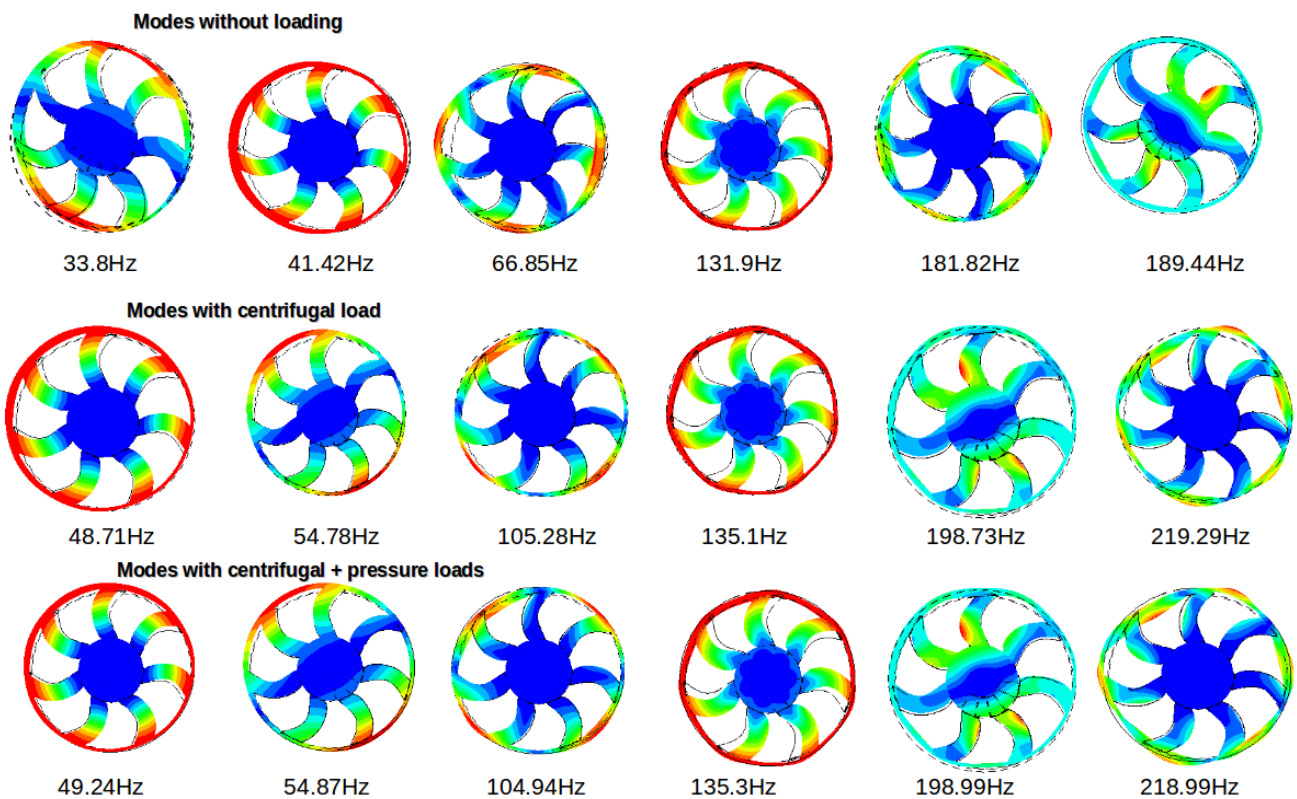


Figure 12: Modes analysis with the centrifugal and the pressure load

DOE AND RESULTS ANALYSIS

The mesh morphing method available in PERMAS [5] software is incorporated into a sampling process in which for each new mesh obtained, static deformation under centrifugal load and modal frequency analysis are performed. The morphing approach thus consists in iterating on the sample database of parameters' set according to design of experiment database provided.

Design of Experiment

Variations of the geometrical parameters on the blades have been provided through two LHS design of experiment, with the 12 parameters previously described and one single rotating speed. An initial sampling of 600 runs is performed for the creation of meta-models, and a second sampling of 300 simulations is used for the validation of the first one. 900 different rotor geometries are then derived from the reference configuration.

Figure 13 shows different shapes out the 900 shapes obtained. The parameterization and the mesh morphing produced smooth transformations in space that preserved the quality of the surface mesh and the global structure mesh. The morphing procedure checks during execution the quality mesh of sampled the structural finite model. It is worthy to notice that variations of some of geometrical parameters have reached up to $\pm 50\%$ of their initial values. This shows the high capability of the finite element model to handle large variations with complex geometries during structural analysis.

The mesh morphing process for the 900 samples with the structural analysis took 25 hours 51 min of calculation on 6-core CPUs. Its means approximately 1 min 44 sec for each run with static and modal analysis computation. The very low computational cost of the morphing combined with the calculation of the linear deformation and modal analysis allow incorporating this procedure into an optimization process with reasonable overall CPU time. However, it does not count the effort for the fluid simulation which is obviously much more important. In order to experiment the DoE methodology, the aerodynamic loading is not taken into account in this test.

Figure 14 shows the graph with the 900 samples indicating displacement for each design and frequency of the first mode. Depending on the set of parameters, the displacement can vary roughly between ± 15 mm and the first mode goes from 30 to 60 Hz.

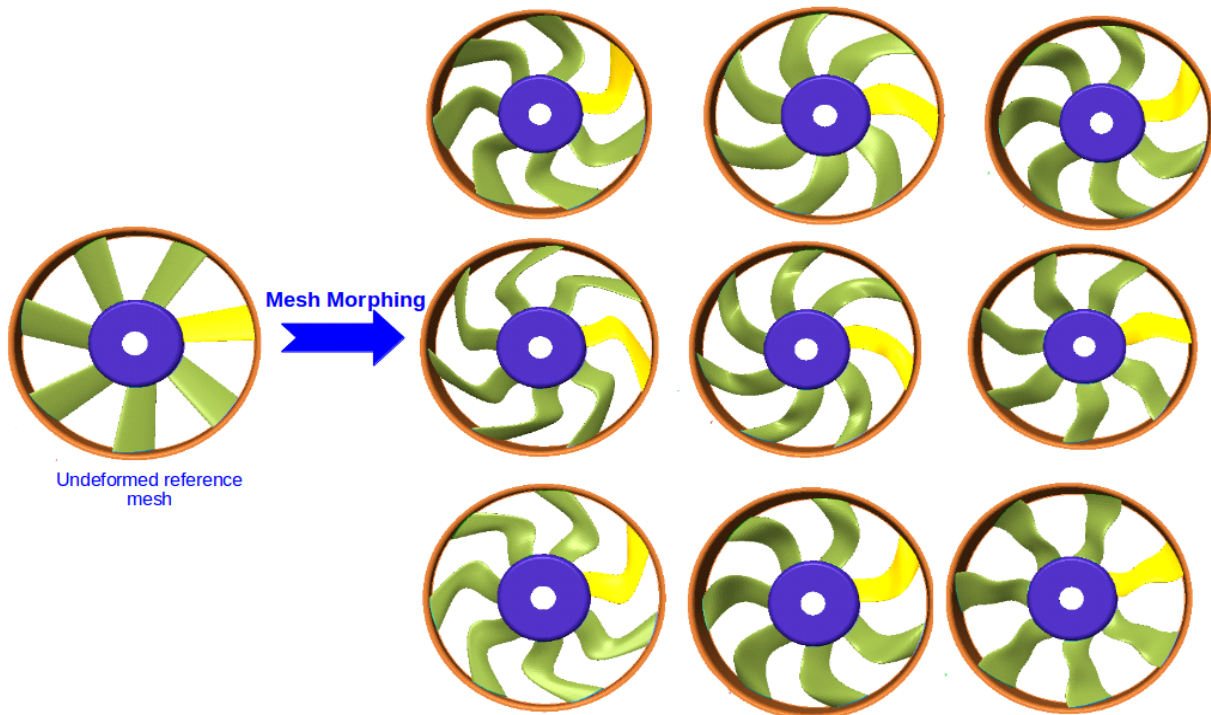


Figure 13: Nine morphing examples out of the 900 runs

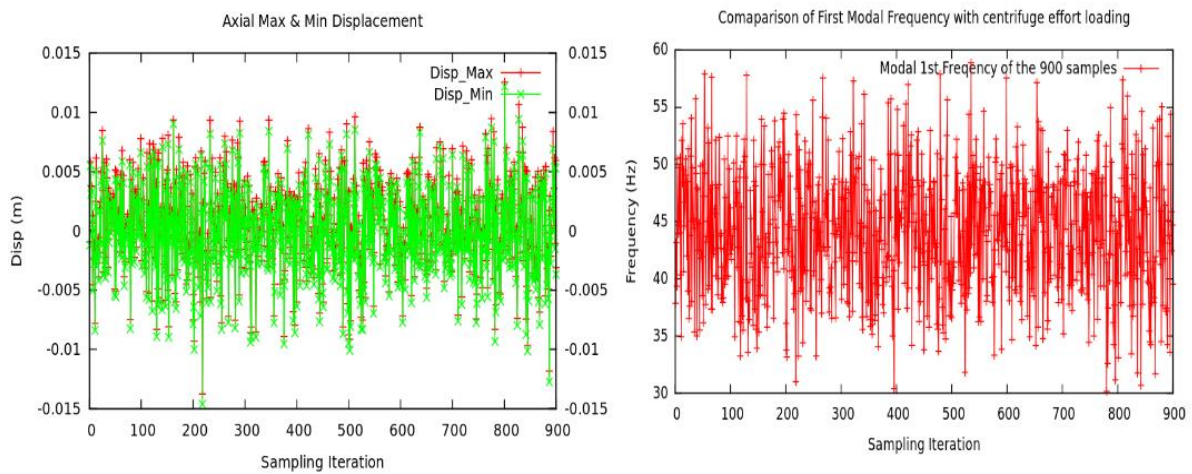


Figure 14: Positive and negative maximum static deformation for the 900 runs (left), first modal frequency (right)

Meta-modeling validation and error assessment

Meta-models for both axial displacement and first mode are created using the radial based function of the commercial code Isight. The surrogated surfaces are deduced from the 600 runs of the initial LHS sampling, and the 300 values of the second LHS are used as test population. The correlations between predictions and these 300 values are presented in figure 15 and 16. Models can be considered at this step as rather satisfying.

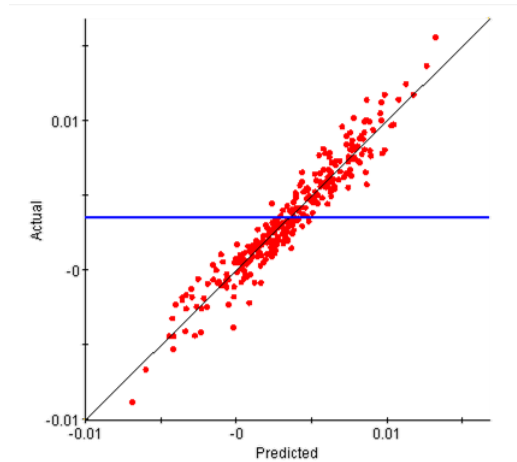


Figure 15: Correlation between meta-model prediction and test population for axial displacement (m)

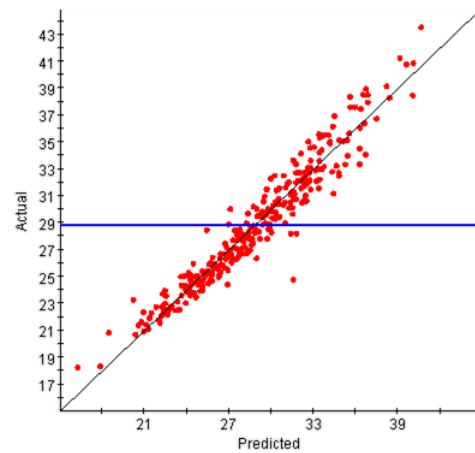


Figure 16: Correlation between meta-model prediction and test population for first mode (Hz)

Further investigations on both model qualities were undertaken using an optimization process for four objectives which were arbitrary defined, even if they have no real interest for fan design. The maximum displacements (positive and negative) were searched, as well as the minimum and maximum first frequencies. First optimizations were performed with a limitation on the parameter range ($\pm 50\%$ of central values) in order to stay in the main core of the domain of solution. Optimizations were then performed with the full parameter range ($\pm 100\%$), allowing to go in some extrema where the meta-models are providing more extrapolation than interpolation.

Results are presented in table 2 with the calculated errors. As expected, it can be observed that meta-models are quite accurate when the parameter range is limited since errors are equal or below 13%. For the full range, it is very interesting to note that the values found are by far above the maximum displacements, or by far below the minimum first frequencies found with the 900 runs. For instance, the minimum frequency found by simulation is only 14 Hz, despite it was never below 30 Hz for the LHS sampling. It highlights the fact that the meta-model is even able to provide good information when searching for poorly unknown area of the domain of solution, and it must be conceded that the accuracy is less good in these cases (up to 75% of error observed).

Parameters	Objectives	Meta-model	Simulation	Errors
Limited range (50%)	Max positive displacement (mm)	8,3	8,1	-2,5%
	Max negative displacement (mm)	-8,7	-7,7	-13,0%
	Max frequency (Hz)	43,4	43,9	1,0%
	Min frequency (Hz)	22,5	22,9	2,0%
Full range (100%)	Max positive displacement (mm)	17,5	14,5	-20,1%
	Max negative displacement (mm)	-20,1	-36,1	44,2%
	Max frequency (Hz)	46,8	44,6	-4,9%
	Min frequency (Hz)	3,6	14,3	75,2%

Table 2: Comparisons of meta-model and simulation predictions

Sensitivity analysis of geometrical parameters

A sensitivity analysis can be done using the results of these study. It reveals the most important parameters to adjust when real optimization objectives are assigned. Average gradients for each of the factors are shown in figure 17 for the displacement, and in figure 18 for the first mode. As the values and the names of the factors are not fully explained for reason of confidentiality, it can be

just remember that stagger angles and sweeps are the most important factors. There are just some permutations between them when looking either the deformation or the modal result.

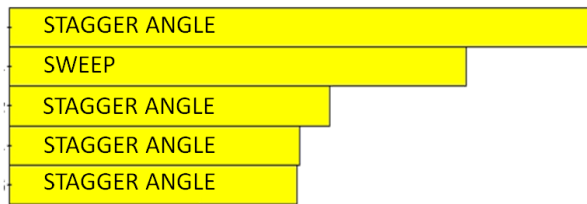


Figure 17: Global effect (averaged gradient)
for displacement

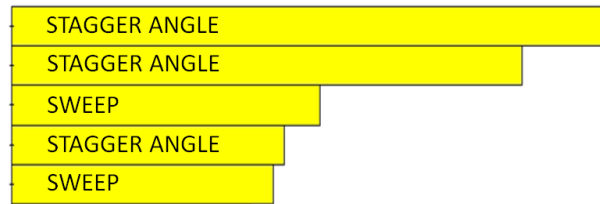


Figure 18: Global effect (averaged gradient)
for first mode

CONCLUSION AND PERSPECTIVES

In the framework of methodological development for multiphysics design of experiment in large dimensions, a tool for the prediction of fan deformation and modal analysis has been tested. The technique is based on a parameterization of the geometry that controls the deformation of the mesh, and it has been successfully tested with 12 parameters having a very large range of variation.

Aerodynamic and structural simulations have shown that a first stationary calculation is sufficient to estimate the aerodynamic load, and that it must be taken into account with the inertial load for the calculation of the fan deformation. Air pressure is however not needed for the modal analysis.

900 sets of parameters were evaluated thanks to the very affordable need for resource with the finite element structural simulation without aerodynamic load so far. Meta-models were build and tested, proving their satisfactory accuracies. The sensitivity analysis showed the importance of both stagger angles and blade sweep.

This methodology will be applied in the future on a 30 parameter DoE with a coupling with CFD results. Taking into account the unsteadiness of the flow could also lead to an analysis of pressure fluctuations and their acoustic radiation with the code PERMAS. Further, a deep stability analysis of the rotor will be conducted to evaluate the complex eigenfrequencies that depend on the rotor rates due to the induced gyroscopic effects by using Campbell diagrams.

ACKNOWLEDGMENT

This work is being supported by the French Research Agency ANR.



BIBLIOGRAPHY

- [1] <http://www.agence-nationale-recherche.fr/Projet-ANR-14-CE23-0011>
- [2] Henner M., Demory B., Franquelin F. and al., “*Test rig effect on performance measurement for low loaded high diameter fan for automotive application*”. ASME Turbo Expo, Frankfurt, Germany, **2014**
- [3] Henner M., Demory B., Moneyron P., “*Acoustic prediction for multi-physic fan optimization*”, ISROMAC 2017, Hawaii, Maui, **2017**

- [4] Rozenberg Y., Aubert S. and Bénédicte G., “*Fluid Structure Interaction Problems in Turbomachinery Using RBF Interpolation and Greedy Algorithm*”, ASME Turbo Expo Düsseldorf, Germany, **2014**
- [5] PERMAS: *Users’ References Manual*, INTES Publication No. 450, Stuttgart, 2010.
- [6] De Boer A., Van der Shoot M. S. and Bijl H., “*Mesh deformation based on radial basis function interpolation*”, *Computers & Structures*, **2007**, 85(11-14), pp. 784-795.
- [7] Kirchgäßner B., “*Finite Elements in Rotordynamics*”, *Procedia Engineering*, pp 736-750, Volume 144, 2016
- [8] Helfrich, R., Wagner N., “*Robust Optimum in Structural Dynamics*”; NAFEMS Seminar: Optimization and Robust Design, 23-24 March 2015, Wiesbaden /Germany
- [9] Goerke D., Schmidt Th., Kocian F., Le Denmat A.-L., Nicke E., “*The application of PERMAS for the design of turbo-machines*”, *Finite Elements in Engineering Applications*, Proceedings of the 11th PERMAS Users’ Conference, Heidelberg, Germany, 26-27 April 2012
- [10] *OpenFOAM User Guide*. Available from : <http://cfd.direct/openfoam/user-guide/>
- [11] Cao Y., Nötzel-Steidle G., Marchesini J., “*Mapping and coupling procedure between PERMAS and OpenFOAM*”; PERMAS Users’ Conference, Stuttgart 2014
- [12] Marchesini J., Helfrich R., Henner M., “*Design of Mechatronic Devices by Electro-Thermal FE Analysis Coupled to CFD Analysis*”; NAFEMS European Conference Multiphysics Simulation, Frankfurt 16-17, Oct 2012